Bioorganic & Medicinal Chemistry 17 (2009) 1928–1937

Contents lists available at ScienceDirect

Bioorganic & Medicinal Chemistry

journal homepage: www.elsevier.com/locate/bmc

5-Arylidene-2-phenylimino-4-thiazolidinones as PTP1B and LMW-PTP inhibitors

Rosaria Ottanà [a,*], Rosanna Maccari [a], Rosella Ciurleo [a], Paolo Paoli [b], Michela Jacomelli [b], Giampaolo Manao [b], Guido Camici [b,†], Christian Laggner [c], Thierry Langer [d]

[a] Dipartimento Farmaco-chimico, University of Messina, Polo Universitario dell'Annunziata, Vl. SS. Annunziata, 98168 Messina, Italy
[b] Dipartimento di Scienze Biochimiche, University of Firenze, Vl. Morgagni 50, 50134 Firenze, Italy
[c] Department of Pharmaceutical Chemistry, Institute of Pharmacy and Center for Molecular Biosciences (CMBI), University of Innsbruck, Innrain 52c, A-6020 Innsbruck, Austria
[d] Prestwick Chemical Inc., Bld. Gonthier d'Andernach, 67400 Strasbourg-Illkirch, France

ARTICLE INFO

Article history:
Received 25 November 2008
Revised 14 January 2009
Accepted 20 January 2009
Available online 25 January 2009

Keywords:
Protein tyrosine phosphatases
PTP1B
LMW-PTP
5-Arylidene-2-phenylimino-4-thiazolidinones
Inhibitors

ABSTRACT

As part of a project aimed at identifying effective low molecular weight nonphosphorus monoanionic inhibitors of PTPs, we have synthesized 4-[(5-arylidene-4-oxo-2-phenyliminothiazolidin-3-yl)methyl]-benzoic acids (**4**) and evaluated their inhibitory activity against human PTP1B and LMW-PTP enzymes. The introduction of a 2-phenylimino moiety onto the 4-thiazolidinone ring was designed to enhance the inhibitor/enzyme affinity by means of further favourable interactions with residues of the active site and the surrounding loops. Some of the compounds (**4a–d**, **f**) showed interesting inhibition levels in the low micromolar range. The 5-arylidene moiety of acids **4** proved to markedly influence the potency of these inhibitors. Molecular modeling experiments inside the binding sites of both enzymes were performed.

1. Introduction

Protein tyrosine phosphorylation is the predominant post-translational modification that cells utilize to regulate signal transduction and to control a wide variety of cellular functions, such as growth, differentiation, survival, apoptosis, metabolism and gene transcription. In vivo it is a reversible and dynamic process which is governed by the coordinated activities of protein tyrosine kinases (PTKs), which catalyse protein phosphorylation, and protein tyrosine phosphatases (PTPs), which are responsible for dephosphorylation.[1–4]

The PTP superfamily comprises more than 100 enzymes.[1–5] PTPs can exert both positive and negative critical effects on various signalling pathways, thus playing complex and important roles in many pathophysiological processes. The deregulation of their activity leads to aberrant tyrosine phosphorylation and is linked to the development of many human pathologies, such as diabetes, obesity, cancer, inflammation and neurodegenerative diseases.[1,3,6] Thus, there is a great interest in PTPs as molecular targets for the development of novel therapeutic agents.

PTP1B is the prototypical member of the PTP superfamily. It is an intracellular enzyme that acts as a key negative regulator of both insulin and leptin signalling pathways. This is achieved by catalysing the dephosphorylation of specific phosphotyrosine (pTyr) residues on insulin receptor, insulin receptor substrate proteins and on Janus kinase 2, a protein tyrosine kinase which is associated with leptin receptors.[7–10]

Inhibition of PTP1B results in both increased insulin sensitivity and resistance to obesity, without producing abnormalities in growth or fertility or other pathogenetic effects in mice.[11,12] This makes PTP1B an exemplary target for obesity and type 2 diabetes (DM2).[7,9,10,13] These two related metabolic pathologies can also be part of the so-called 'metabolic syndrome' which currently represents a serious health threat.[14] Increasing concern about the widespread diffusion of these diseases has led to intensive efforts to develop new drugs that are able to counteract insulin resistance, which is the biochemical defect underlying both DM2 and metabolic syndrome.[14] Indeed, insulin resistance is not sufficiently targeted by the current therapies. Therefore, inhibition of PTP1B is predicted to provide a novel strategy to fill this therapeutic gap.

There is evidence that PTP1B can also play an oncogenic role. It is overexpressed in certain types of human cancer, such as breast tumours, ovarian and epithelial carcinomas, and can act as a positive regulator of tumour onset and progression. PTP1B has been shown to play an important role as a positive regulator of

* Corresponding author. Fax: +39 90 6766402.
E-mail address: ottana@pharma.unime.it (R. Ottanà).
† Address: Centro di Ricerca, Trasferimento ed Alta Formazione DENOThe, University of Firenze, Italy.

0968-0896/$ - see front matter © 2009 Elsevier Ltd. All rights reserved.
doi:10.1016/j.bmc.2009.01.044

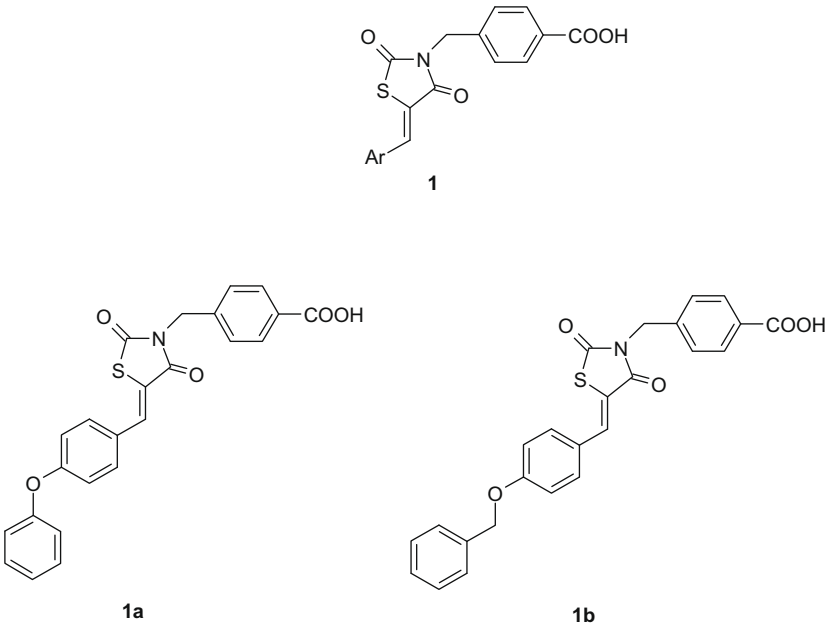

Figure 1. Structures of previously reported inhibitors.[32]

the Erb2-PTK, which is overexpressed in several human breast cancers that are difficult to treat. PTP1B deficiency or inhibition delays Erb2-induced tumourogenesis and protects from lung metastasis.[3,10,15,16]

Low molecular weight PTP (LMW-PTP), which possesses a phosphate binding loop structurally identical to that of PTP1B, also acts as a negative regulator of insulin mediated mitotic and metabolic signalling.[10,17,18] Recently, Pandey reported that the reduction of LMW-PTP expression (both in vitro and in vivo), using a specific antisense oligonucleotide, induces increased phosphorylation and activity of key insulin signalling intermediates in response to insulin stimulation.[19] Analogously to PTP1B, it has also been shown to be a possible positive factor in tumour development. High levels of this PTP have been detected in breast and colon tumours and neuroblastoma.[20–22] Consequently, both PTP1B and LMW-PTP are attractive targets for the development of new antidiabetic and antitumour agents.

Although a variety of PTP1B inhibitors have been reported in the last decade,[7,10,13,23] the identification of selective, safe and orally available inhibitors of these PTPs has proven difficult and it still represents a challenge for medicinal chemists.

In the search for active site PTP inhibitors, a valid method to obtain compounds with low polarity is to replace the phosphate group of pTyr with nonhydrolysable monoanionic bioisosteres, such as carboxylates.[13,24–26] This may prevent the pharmacokinetic limitations of certain highly charged pTyr mimetics, such as phosphonate, which have often been utilized to obtain potent in vitro PTP1B inhibitors.[3,7,10,13] Indeed, several carboxylic acids with good PTP1B inhibitory profiles and cellular activity or oral bioavailability have been reported.[25,27–31]

We have recently reported a series of 4-[(5-arylidene-2,4-dioxothiazolidin-3-yl)methyl]benzoic acids (**1**) (Fig. 1) that we have designed and evaluated as PTP1B and LMW-PTP inhibitors. They were shown to be competitive and reversible PTP inhibitors, with an appreciable selectivity towards human PTP1B and IF1 isoform of human LMW-PTP compared with other related PTPs.[32]

In the structure of compounds **1**, the *p*-methylbenzoic acid residue was inserted as a nonphosphorus monoanionic pTyr-mimic onto N-3 of the 2,4-thiazolidinedione ring. It proved to be an effective pTyr-mimetic group that is able to replicate the interactions of pTyr residue with the catalytic sites of both PTP1B and LMW-PTP.[32]

The 5-arylidene moiety of acids **1**, which was inserted in order to improve the stability of the inhibitor/enzyme complex through contacts with residues bordering the active site, proved to markedly influence the potency and selectivity of these inhibitors. In particular, inhibitory effectiveness, especially towards PTP1B and IF1, was shown to be enhanced by a larger lipophilic 5-arylidene moiety containing two aromatic rings rather than by a smaller one composed of a hydroxysubstituted benzylidene ring.[32]

Compounds **1a** and **1b** (Fig. 1) were found to be the most effective inhibitors of both human PTP1B and IF1. Moreover, molecular docking experiments into the PTP1B active site indicated that the 4-phenoxybenzylidene and 4-benzyloxybenzylidene moieties of compounds **1a** and **1b** fitted a second noncatalytic arylphosphate binding site very well by establishing favourable hydrophobic interactions and hydrogen bonds. This secondary pocket is not conserved among all PTPs and thus provides a structural basis for selective PTP1B inhibition.[10,33,34] These findings were in agreement with our in vitro inhibition results. In particular **1a** and **1b** exhibited good activity towards PTP1B as well as towards other related PTPs containing this pocket (such as TC-PTP, YopH, PTPβ), whereas their inhibitory effect was lower (10–20-fold) against LAR-PTP, a transmembrane receptor-like PTP which does not contain the second arylphosphate binding site.[32]

In continuing our search for PTP1B and LMW-PTP inhibitors, we designed analogous 4-[(5-arylidene-4-oxo-2-phenyliminothiazolidin-3-yl)methyl]benzoic acids (**4**) (Fig. 2) with the aim of improving the inhibitory effects of acids **1**.

We wanted to test the hypothesis whether replacing the carbonyl group in position 2 of the 2,4-thiazolidinedione scaffold with a phenylimino moiety could enhance the inhibitor/enzyme affinity by means of further favourable interactions with residues of the active site and the surrounding loops, particularly with the WPD loop (residues 179–189). This flexible loop, which forms one edge of the PTP1B catalytic pocket, contributes to substrate and inhibitor affinity and specificity. In the absence of substrate the WPD loop is in an 'open' conformation and closes down on the side chain of pTyr residue upon substrate binding. This conformational change is required for catalysis. Thus, inhibitors which reduce

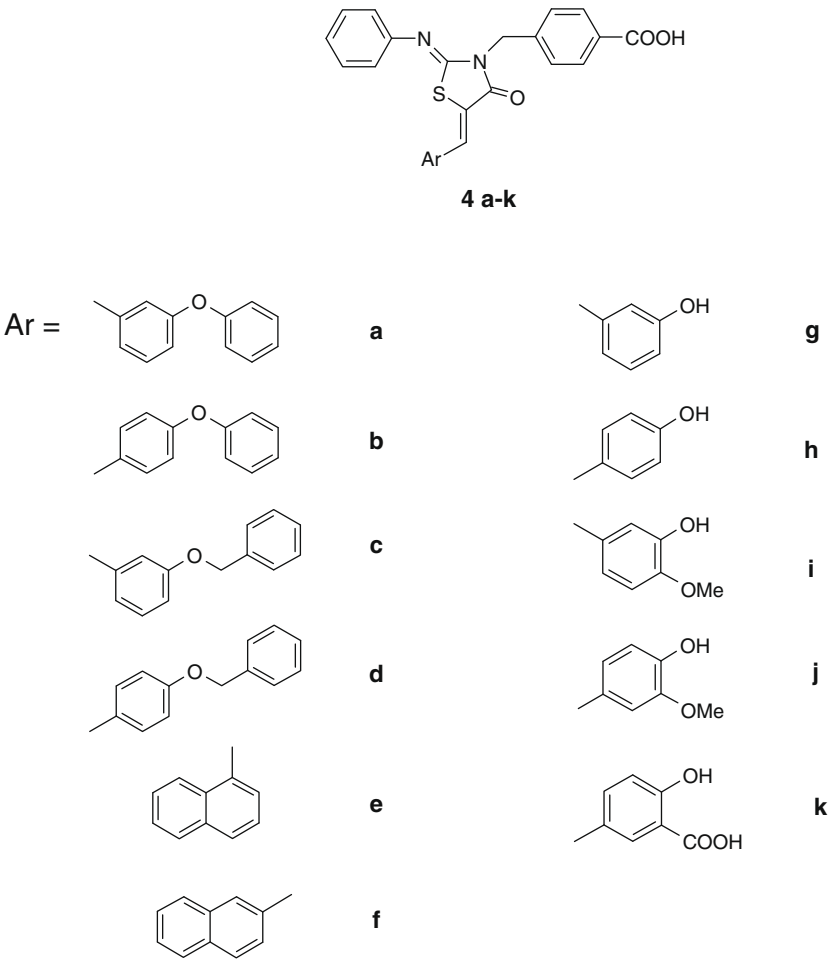

Figure 2. Structures of compounds **4a–k**.

the mobility of WPD loop may prevent substrate binding especially when they bind the enzyme in the closed conformation.[4,10]

The insertion of the phenylimino moiety in position 2 of the pentatomic scaffold also enhances the hydrophobic character of the compounds. Considering that it is important to include at least one monoanionic functionality in the structure of PTP inhibitors in order to obtain electrostatic driving forces for efficacious binding with the catalytic phosphate binding site of these enzymes, the introduction of lipophilic moieties in the structure of such inhibitors can represent a good general approach to improve their cell permeability.[10,13]

Compounds **4a–k** were evaluated for their in vitro inhibitory activity against recombinant human PTP1B as well as the two active isoforms of human LMW-PTP (IF1 and IF2) and *Saccharomyces cerevisiae* LMW-PTP (Ltp1).

2. Chemistry

(*Z*)-4-[(5-Arylidene-4-oxo-2-phenyliminothiazolidin-3-yl)methyl]benzoic acids (**4**) were synthesized following the synthetic pathway described in Scheme 1.

The intermediate 4-(3-phenylthioureidomethyl)benzoic acid (**2**) was obtained by the reaction of phenylisothiocyanate and 4-(aminomethyl)benzoic acid in ethanol at reflux.

The subsequent synthesis of 4-[(4-oxo-2-phenyliminothiazolidin-3-yl)methyl]benzoic acid (**3**) was performed by condensation of compound **2** with chloroacetyl chloride in the presence of triethylamine as base in ethanol at reflux for 24 h. In these experimental conditions compound **3** is the only isomer obtained from N-aryl-N'-alkyl-substituted thioureas, as previously reported.[35] In fact, when the reaction was carried out in $CHCl_3$ at room temperature both 2-phenylimino and 2-benzylimino isomers were obtained; they arose from the condensation of chloroacetyl chloride and two possible intermediate ene-thiols generated by the delocalization of the lone pairs of the two different nitrogen atoms on the adjacent thiocarbonyl group.[35]

The condensation of compound **3** with the appropriate aromatic aldehydes, using piperidine as base in refluxing ethanol for 96 h, provided compounds **4a–k**. The reaction time was significantly reduced (6 h) by using microwave irradiation (200 psi, 300 W maximum power) at 140 °C.

The introduction of 5-arylidene moiety provided only *Z* isomers, as already demonstrated by X-ray diffraction studies.[35,36]

The structure of all compounds was unambiguously assigned by means of analytical and ^1H and ^{13}C NMR spectroscopy data.

In ^1H NMR spectrum of compounds **3**, the signal of NCH_2 protons as well as the analogy of previously reported compounds[32,35] allowed us to identify the structure of the 3-(4-carboxy)benzyl-2-phenylimino isomer. The above mentioned protons appeared as a singlet resonating at chemical shift ranging between 5.26 and 4.92 ppm, due to the deshielding effect generated by the extended electronic delocalization of the 3-N lone pair on the highly conjugated system. In fact, in the case of the 2-(4-carboxy)benzyl-3-phenylimino isomer the $N–CH_2$ protons should resonate at lower chemical shifts.[35]

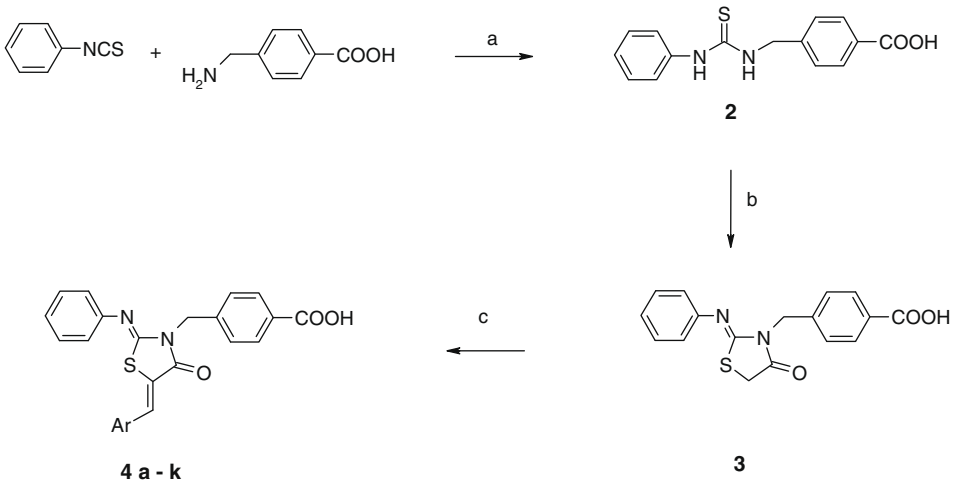

Scheme 1. Reagents and conditions: (a) EtOH, Δ; (b) $ClCH_2COCl$, Et_3N, EtOH, Δ; (c) ArCHO, $C_5H_{11}N$, EtOH, Δ.

The disappearance of the 5-CH_2 signal of compound **3** as well as the presence of the methylidene proton at 7.70–8.56 ppm were determinant in assigning the structure of compounds **4**. ^{13}C spectra showed a clear change in the splitting pattern of 5-C which resonated as a triplet at 32.70 ppm in **3** and as a singlet in the range 118.3–126.4 ppm in compounds **4**.

3. Results and discussion

Table 1 shows the results of inhibition levels of 4-[(5-arylidene-4-oxo-2-phenyliminothiazolidin-3-yl)methyl]benzoic acids (**4a–k**), expressed as IC_{50} (μM), against recombinant human PTP1B, the two active IF1 and IF2 isoenzymes of human LMW-PTP as well as *S. cerevisiae* LMW-PTP (Ltp1). The *p*-nitrophenylphosphate was used as substrate.

All compounds proved to be good reversible inhibitors of human PTP1B and LMW-PTP, exhibiting IC_{50} values in the micromolar range. We determined also the inhibition type analyzing experimental data of some effective inhibitors of PTP1B (compounds **4b**, **4d** and **4f)** by the double reciprocal plot method. The initial hydrolysis rate using eight substrate final concentrations (0.5–40 mM range) was measured in the presence of increasing concentrations of each compound. All reciprocal plots display straight lines that intersect each other in the 1/v axis, suggesting that they are competitive type inhibitors. In fact the increasing inhibitor concentration is accompanied by the increase of K_m values and by very close values of V_{max} (see Supplementary data).

Compounds **4b** and **4d**, 4-phenoxy- and 4-benzyloxybenzylidene substituted, were the most effective inhibitors as they achieved interesting inhibition levels against both human PTP1B (IC_{50} = 1.1 μM) and IF1 isoform of LMW-PTP (IC_{50} = 3.1 and 2.7 μM, respectively) while their inhibitory effectiveness was found to be lower towards IF2 isoform and Ltp1 (Table 1). They were slightly more active towards PTP1B in comparison with compounds **1a** and **1b** (IC_{50} = 2.8 and 1.6 μM, respectively).[32]

The displacement of both 4-phenoxy and 4-benzyloxy groups to position 3 of the 5-benzylidene moiety gave access to compounds **4a** and **4c**, respectively, which exhibited an interesting enzymatic inhibition profile particularly against PTP1B (IC_{50} = 1.9 and 3.8 μM) and IF1 (IC_{50} = 5.4 and 3.1 μM) without reaching the inhibition levels of the 4-substituted analogues. In comparison with the 5-arylidene-2,4-thiazolidinedione analogues they proved to be generally more active towards all enzymes, except in the case of **4c** that was about 3-fold less effective against PTP1B.

Compound **4a** was shown to be 10-fold more active than 4-{[2,-4-dioxo-5-(3-phenoxybenzylidene)thiazolidin-3-yl]methyl}benzoic acid towards human PTP1B and from 5- to 7-fold against IF1 and IF2.[32]

A 5-naphthalenylmethylene group was inserted in order to expand the 5-arylidene moiety, thereby providing compounds **4e** and **4f** (5-naphthalen-1-yl)methylene and (5-naphthalen-2-yl)methylene substituted. Compound **4f** maintained good inhibition levels against both human PTP1B and IF1 LMW-PTP and proved to be more active than both the corresponding 2,4-thiazolidinedione and compound **4e** against all tested PTPs. The latter compound was shown to be 7-fold less active against PTP1B and 4-fold against IF1 than **4f**.

Molecular docking experiments as well as the PTP inhibitory activity of 4-[(5-arylidene-2,4-dioxothiazolidin-3-yl)methyl]benzoic acids (**1**) had indicated that a second aromatic ring on 5-arylidene moiety promoted the activity.[32] This beneficial effect most likely derived from its ability to interact with the secondary pocket of PTP1B by enabling it to reach the most remote aminoacids (Ala27, Met258, Gly259, Arg24). In fact, the replacement of the phenoxy and benzyloxy groups on 5-arylidene with a hydroxy group that is able to establish different interactions resulted in lower inhibitory activity.[32]

A similar pattern was observed in compounds **4g–k**, which were shown to be significantly less active than both analogous compounds **4a–d** and corresponding 5-arylidene-2,4-thiazolidinediones **1**. Indeed, 3-hydroxy- and 4-hydroxybenzylidene derivatives (**4g** and **4h**, respectively) were from 10-fold to 30-fold less active towards PTP1B and IF1 and 30-fold less active towards IF2 and Ltp1 compared with derivatives **4a–d**.

The introduction of a methoxy group in the *para* or *meta* positions of hydroxybenzylidene moiety of compounds **4g** and **4h** provided derivatives **4i** and **4j**, respectively; these modifications did not result in any change in the levels of inhibitory activity.

Among compounds **4g–k** bearing a hydroxy group on 5-benzylidene moiety, compound **4k**, 5-(3-carboxy-4-hydroxy)benzylidene substituted, was shown to be the most active against both PTP1B (IC_{50} = 19.5 μM) and IF1 (IC_{50} = 43.1 μM). However, it was less active than compounds bearing two aromatic rings in the 5-arylidene moiety.

The generally increased affinity of compounds **4** towards Ltp1 in comparison with compounds **1** may be determined by the 2-phenylimino moiety which extends the surface contact between the inhibitors and hydrophobic residues lining the deep active site cavity of the enzyme.[37] In fact, among compounds **4**, the most lipophilic derivatives (**4a–d**, **4f**) reached good inhibition levels towards Ltp1.

Table 1
In vitro inhibition activity of compounds **4a**–**k** against human PTP1B, IF1 and IF2 isoforms of human LMW-PTP and LMW-PTP (Ltp1) from *S. cerevisiae*[a]

Ar	Compound	IC_{50} (μM)			
		PTP1B	IF1	IF2	Ltp1
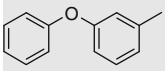	**4a**	1.9 ± 1.0	5.4 ± 0.5	26.1 ± 1.7	11.1 ± 0.6
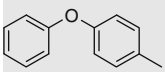	**4b**	1.1 ± 0.1	3.1 ± 0.4	8.2 ± 0.3	6.3 ± 0.2
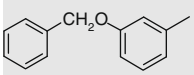	**4c**	3.8 ± 0.1	3.1 ± 0.5	12.1 ± 0.5	12.9 ± 0.1
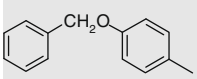	**4d**	1.1 ± 0.1	2.7 ± 0.2	21.5 ± 2.2	15.9 ± 2.2
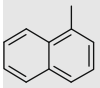	**4e**	14.0 ± 1.0	16.1 ± 1.8	1004 ± 99	>500
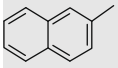	**4f**	1.9 ± 0.1	3.7 ± 0.2	13.8 ± 0.8	27.6 ± 3.2
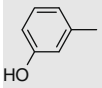	**4g**	35.4 ± 3.0	62.5 ± 1.6	>250	>250
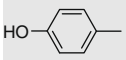	**4h**	30.1 ± 3	47.7 ± 1.6	269.7 ± 1.5	195.4 ± 5.6
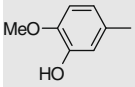	**4i**	32.1± 3.6	87.1 ± 9.2	>250	>250
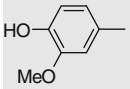	**4j**	33.7 ± 8.0	71.2 ± 1.5	>250	>250
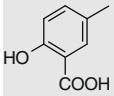	**4k**	19.5 ± 0.8	43.1 ± 3.1	389.0 ± 35	344.9 ± 38

[a] IC_{50} values were determined by regression analyses and expressed as means ± SE of three replicates.

For our docking studies, PDB structures 1G7F, 1G7G[38] and 1XBO[29] were selected as templates for human PTP1B. PDB structures 5PNT[39] and 1XWW[40] were selected as templates for human LMW-PTP IF1 and IF2, respectively. Structures 1G7F and 1G7G have similar ligands, but in 1G7F the WPD loop is in its open form, whereas in 1G7G, as like in most of the reported protein–ligand complex structures for PTP1B, it is closed. In both structures, the main axis of the ligand is oriented towards the wall formed by residues Asn42 to Arg47, whereas in 1XBO, which is also a 'closed' structure, the main axis of the ligand reaches deeper into the secondary pocket lined by residues Arg24 to Lys36 and this is the one we previously predicted to be the relevant one for compounds **1**.[32] The selected protein structures were processed in Maestro (Schrödinger, LLC)[41] using the Protein Preparation Wizard. All water molecules were removed from the protein structure. The Induced Fit Docking (IFD) protocol developed by Schrödinger, LLC, which takes into account the flexibility of the binding site, was used for docking our compounds.[42,43] This approach seemed reasonable because in both PTP1B and LMW-PTP flexible side chains of multiple residues reach into the binding site. Based on the ligand from 5PNT, identical box sizes were chosen for LMW-PTP.[39] The enclosing box size was enlarged to 30 Å for all investigated structures. All other values of the IFD protocol were kept at their default values.

We selected compounds **4a**, **4b**, **4e**, **4f** and **4h**, a diverse sample of compounds with different shapes and polarities, for docking experiments. In addition, their respective analogues from series **1** were docked in order to detect any possible differences between the two series. All compounds were drawn and minimized using Maestro. The carboxylic acid groups of the ligands were always drawn in their deprotonated form.

Docking in 1G7F resulted in poses that were largely in agreement with our previous predictions, with the carboxylate group positioned at the phosphate binding region, and the distal groups stretching into the secondary non-catalytic hydrophobic pocket. Only weak interactions of the phenylimino group with Arg24 (π–π stacking) and Thr263 (hydrophobic) could be detected. No favourable interaction with the open WPD loop were found. In fact, the open conformation of 1G7F moves the lipophilic side chain of Phe182 away from the position where it can set up hydrophobic interactions with the phenylimino group of the ligands. In 1G7G, we found many poses where the caboxylate group interacts with the basic center formed by Arg24, Arg254 and Tyr20, leaving the primary phosphate binding region occupied by the distal ligand residues. The analysis of available X-ray structures of PTP1B shows these poses to be unlikely, since the presence of an acidic group at the phosphate binding region seems to be a prerequisite for ligand-binding. In 1XBO (Fig. 3), **4b** is more consistently placed in a posi-

tion where the phenoxyphenyl residue is placed in the hydrophobic secondary pocket. The phenylimino group makes hydrophobic interactions with either Phe182 or with Tyr 46. In the first case, a π-cation interaction can be perceived between Arg24 and the three phenyl groups from the phenylimino and phenoxybenzylidene residues, which surround at a distance of about 4–6 Å, whereas in the second proposed orientation, the phenylimino group appears to stack with an intramolecular salt-bridge formed by side-chain residues of Arg47 and Asp48. For shorter molecules **4e**, **4f** and **4h**, no consistent pose preferences were obtained.

Docking into the two LMW-PTP binding sites gave more consistent results over the series of investigated compounds, especially for IF2 (1XWW). The preferred pose for all compounds, both from series **1** and **4**, is the one in which the carboxylic group is placed in the phosphate-binding region through charged interactions with Arg18 and also by receiving hydrogen bonds from Cys12, Leu13, Cys17 and Arg18. The thiazolidinone ring is stacked with the indole ring of Trp49, and is held by hydrogen bonds between the phenolic group of Tyr132 and the oxygen of the carbonyl group in position 2 (compounds **1**) or the 2-imino nitrogen atom (compounds **4**), and between the amide side chain nitrogen atom of Asn50 and the carbonyl group in position 4 (Fig. 4). The aromatic residues of the 5-arylidene and phenylimino groups fold slightly around the indole ring of Trp49, making hydrophobic and maybe also slightly off-plane π–π interactions. Again, additional hydrophobic interactions of the phenylimino group contribute to their improved affinity (Fig. 4, right side). IF1 has Glu instead of Asn at position 50, leading to the loss of one possible hydrogen bond donor. The other difference in the binding site is the replacement of Trp with Tyr at position 49, which again is embraced by the thiazolidine residue and its double-bonded phenylimino and 5-arylidene moieties in poses obtained for **4a** and **4b** (Fig. 4, left side). However, for the shorter molecules (**4e**, **4f**, **4h**) as well as for the 2,4-thiazolidinediones Tyr49 is moved outwards, placing the thiazolidinone ring between the aromatic ring of Tyr49 and the isobutyl chain of Leu13. However, since the arylidene part does not interact with the protein this pose appears as unlikely. A hydrogen-bond is detected between Tyr131 and the carbonyl group in position 4 of the ligand, while the 2-phenylimino group is too far away from Tyr132 for a hydrogen bond to form. In both isoforms, the distal phenoxy group interacts only weakly, if at all, with the protein surface.

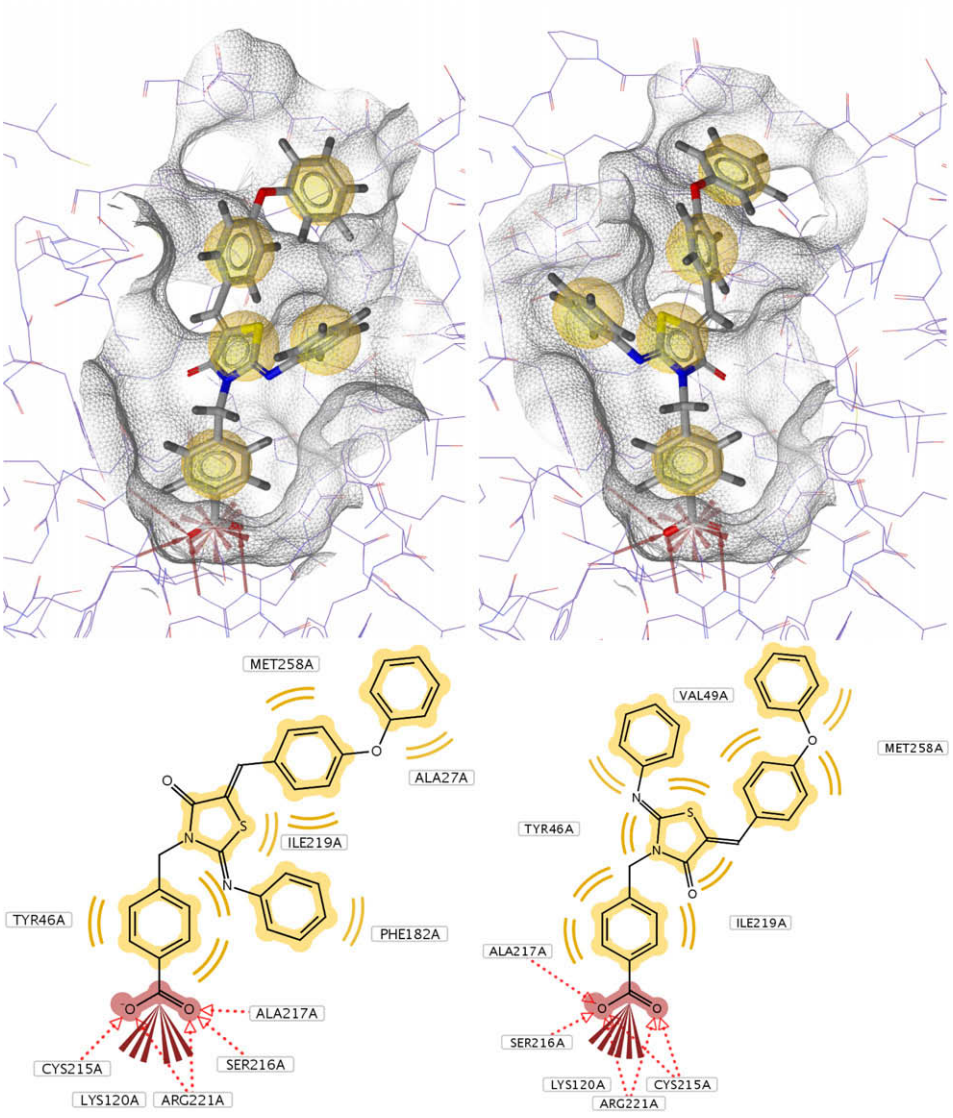

Figure 3. Main docking poses received for **4b** in PTB1B (PDB structure 1XBO.[39] Top: 3D representation, bottom: 2D representation. Pharmacophoric interactions were automatically detected by LigandScout.[44] Yellow sphere: hydrophopic feature; red arrow: hydrogen bond acceptor; red star: negative ionizable feature.

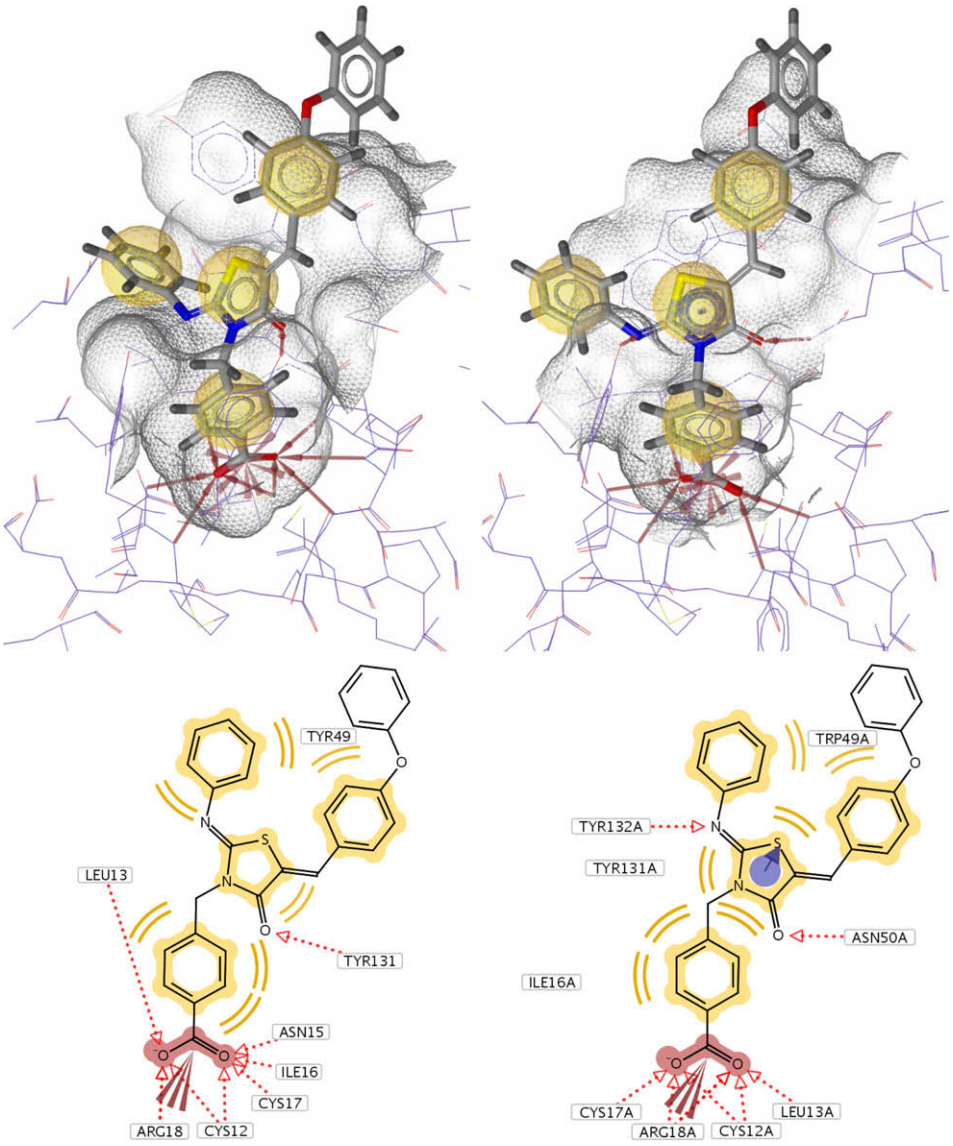

Figure 4. Main docking poses received for **4b** in LMW-PTP IF1 (PDB code 5PNT,[39] left) and IF2 (PDB code 1XWW,[40] right). Top: 3D representation, bottom: 2D representation. Pharmacophoric interactions were automatically detected by LigandScout.[44] Yellow sphere: hydrophopic feature; red arrow: hydrogen bond acceptor; red star: negative ionizable feature; purple ring and arrow: aromatic feature. For IF2, the surface accessibility threshold value was lowered from 250 to 130 to detect the hydrophobic interaction of the benzylidene ring.

4. Conclusions

The design and the synthesis of 4-[(5-arylidene-4-oxo-2-phenyliminothiazolidin-3-yl)methyl]benzoic acids (**4**) are part of a project that aims to identify new nonphosphorus monoanionic PTP1B and LMW-PTP inhibitors.

Compounds **4a–d, 4f** appeared to possess the highest inhibitory activity levels against both human PTP1B and IF1 isoform of human LMW-PTP in the low micromolar range, while they were relatively moderate inhibitors of IF2 isoform and Ltp1 from *S. cerevisiae.*

The SARs that were previously acquired with 2,4-thiazolidinediones derivatives were found to be retained in compounds **4**. A large lipophilic arylidene moiety in position 5 particularly favoured the activity; phenoxy and benzyloxy groups both in the *para* and *meta* positions of the 5-benzylidene group gave the best levels of enzyme inhibition. The removal of the second aromatic ring and its replacement with hydrophilic groups led to a significant decrease in the inhibitory potency.

On the whole, comparing the inhibitory effects of these 2-phenylimino-4-thiazolidinones with those of their 2,4-thiazolidinedione analogues highlighted that some phenylimino derivatives (**4a**, **4b**, **4f**) with a 5-arylidene moiety containing two aromatic rings, had higher potency against PTP1B and/or IF1. In contrast, hydroxybenzylidene substituted analogues were found to be less effective than the corresponding thiazolidinediones.

In our docking experiments, we were able to detect additional hydrophobic interactions of the introduced phenylimino group in PTP1B, IF1 and IF2, which is consistent with the improved affinities of derivatives **4a** and **4b** in comparison with the corresponding analogues **1**. For PTP1B, the possible ligand orientation presented in our previous paper still appears plausible, while other orientations—especially for smaller compounds **4e**, **4f**, **4h—** cannot be ruled out. The binding site of PTP1B is large, open and lined with flexible side chains, making it difficult to predict the binding pose. Although we obtained poses that look very plausible for LMW-PTP IF2 we are unable to explain the generally higher affinity of our compounds towards IF1.

5. Experimental

5.1. Chemistry

Melting points were recorded on a Kofler hot-stage apparatus and are uncorrected. TLC controls were carried out on precoated silica gel plates (F 254 Merck). Elemental analyses (C, H, N), determined by means of a C. Erba mod. 1106 elem. Analyzer, were within ±0.4% of theory. ^{1}H and ^{13}C NMR spectra were recorded on a Varian 300 magnetic resonance spectrometer (300 MHz for ^{1}H and 75 MHz for ^{13}C). Chemical shifts are given in δ units (ppm) relative to internal standard Me_4Si and refer to DMSO-d_6 solutions. Coupling constants (J) are given in hertz (Hz). ^{13}C NMR spectra were determined by Attached Proton Test (APT) experiments and the resonances were always attributed by proton–carbon heteronuclear chemical shift correlation.

Unless stated otherwise, all materials were obtained from commercial suppliers and used without further purification.

5.1.1. Synthesis of 4-[(3-phenyltioureido)methyl]benzoic acid (2)

A mixture of phenylisothiocyanate (0.35 g, 2.6 mmol) and 4-(aminomethyl)benzoic acid (0.5 g, 3.3 mmol) in ethanol was refluxed for 24 h. The solvent was evaporated under vacuo and the solid residue was crystallized from methanol providing compound **2**.

Yield 100%; mp 223–225 °C; ^{1}H NMR ($CDCl_3$): δ 4.80 (d, J = 5.7 Hz, 2H, NCH_2); 7.07 (m, 2H, arom); 7.32–7.42 (m, 5H, arom); 7.89 (m, 2H, arom); 8.30 (br s, 1H, CH_2NH); 9.75 (br s, 1H, NH); 11.00 (br s, 1H, COOH); ^{13}C NMR (DMSO-d_6): δ 47.4 (CH_2); 124.0, 124.9, 127.8, 129.2, 129.9 (CH arom); 130.0, 139.7, 144.9 (Cq arom); 167.8 (C=O); 181.6 (C=S). Anal. Calcd for $C_{15}H_{14}N_2O_2S$: C, 62.92; H, 4.93; N, 9.78. Found: C, 63.18; H, 4.73; N, 10.01.

5.1.2. Synthesis of 4-[(4-oxo-2-phenyliminothiazolidin-3-yl)methyl]benzoic acid (3)

A mixture of **2** (0.5 g, 1.7 mmol) and triethylamine (0.52 g, 5.1 mmol) in ethanol (50 ml) was maintained at reflux for 30 min. A solution of chloroacetic chloride (0.28 g, 2.5 mmol) in ethanol (10 ml) was added and the mixture was refluxed for 24 h. After evaporation of the solvent under reduced pressure, the crude solid was dissolved in $CHCl_3$ and the solution was washed with water. The evaporation of the solvent under reduced pressure and the recrystallization from methanol provided pure compound **3**. Yield 70%; mp 165 °C; ^{1}H NMR ($CDCl_3$): δ 3.88 (s, 2H, 5-CH_2); 5.14 (s, 2H, NCH_2); 6.96 (d, J = 7.5 Hz, 2H, arom); 7.18 (dd, J = 7.5 and 7.5 Hz, 1H, arom); 7.37 (dd, J = 7.5 and 7.5 Hz, 2H, arom); 7.60 (m, 2H, arom); 8.09 (m, 2H, arom); ^{13}C NMR ($CDCl_3$): δ 32.7 (5-CH_2); 46.0 (NCH_2); 120.9, 124.8, 128.9, 129.3, 130.4 (CH arom); 141.6, 147.5 (Cq arom); 153.8 (C=N); 171.0, 171.6 (C=O). Anal. Calcd for $C_{17}H_{14}N_2O_3S$: C, 62.56; H, 4.32; N, 8.58. Found: C, 62.68; H, 4.17; N, 8.71.

5.1.3. General method for the synthesis of 4-[(5-arylidene-4-oxo-2-phenyliminothiazolidin-3-yl)methyl]benzoic acids (4a–k)

A mixture of 4-[(4-oxo-2-phenyliminothiazolidin-3-yl)methyl]-benzoic acid **3** (0.5 g, 1.5 mmol), appropriate aldehyde (1.5 mmol) and piperidine (0.26 g, 3 mmol) in ethanol (50 ml) was refluxed for 96 h. The solution was poured in water acidified with glacial acetic (pH 3–4); the crude solid was washed with H_2O and recrystallized from methanol providing pure acids **4**.

5.1.4. 4-{[4-Oxo-5-(3-phenoxybenzylidene)-2-phenyliminothiazolidin-3-yl]methyl}benzoic acid (4a)

Yield 19%; mp 219–223 °C; ^{1}H NMR ($CDCl_3$): δ 5.23 (s, 2H, NCH_2), 6.94–7.43 (m, 14H, arom); 7.61 (m, 2H, arom); 7.72 (s, 1H, CH); 8.08 (m, 2H, arom); ^{13}C NMR ($CDCl_3$): δ 46.0 (NCH_2), 118.5, 119.4, 119.5, 120.9, 123.9, 124.3, 124.8, 128.4, 129.2, 129.7, 129.9, 130.2, 130.5 (CH arom and CH methylidene); 122.2 (5-C); 130.3, 135.1, 140.4, 147.6, 155.9, 158.1 (Cq arom); 149.5 (C=N); 166.3, 166.9 (C=O). Anal. Calcd for $C_{30}H_{22}N_2O_4S$: C, 71.13; H, 4.38; N, 5.53. Found: C, 71.27; H, 4.52; N, 5.38.

5.1.5. 4-{[4-Oxo-5-(4-phenoxybenzylidene)-2-phenyliminothiazolidin-3-yl]methyl}benzoic acid (4b)

Yield 43%; mp 249–252 °C; ^{1}H NMR ($CDCl_3$): δ 5.26 (NCH_2); 7.01–7.42 (m, 14H, arom); 7.64 (m, 2H, arom); 7.78 (s, 1H, CH); 8.11 (m, 2H, arom); ^{13}C NMR (DMSO-d_6): δ 46.0 (NCH_2); 118.9, 120.1, 121.4, 124.9, 125.3, 128.1, 129.9, 130.0, 130.7, 130.8, 132.5 (CH arom and CH methylidene); 119.7 (5-C); 128.4, 130.5, 141.4, 148.0, 150.0, 158.9 (Cq arom); 150.0 (C=N); 166.2, 167.5 (C=O). Anal. Calcd for $C_{30}H_{22}N_2O_4S$: C, 71.13; H, 4.38; N, 5.53. Found: C, 71.02; H, 4.28; N, 5.67.

5.1.6. 4-{[5-(3-Benzyloxybenzylidene)-4-oxo-2-phenyliminothiazolidin-3-yl]methyl}benzoic acid (4c)

Yield 23%; mp 256–258 °C; ^{1}H NMR ($CDCl_3$): δ 4.92 (s, 2H, NCH_2); 5.07 (s, 2H, OCH_2); 6.85–7.25 (m, 14H, arom); 7.42 (m, 2H, arom); 7.57 (s, 1H, CH); 7.88 (m, 2H arom); ^{13}C NMR ($CDCl_3$): δ 44.7 (NCH_2); 68.7 (OCH_2); 114.8, 115.6, 119.8, 121.3, 123.8, 126.2, 126.8, 127.0, 127.3, 128.2, 128.7, 129.0, 129.9 (CH arom and CH methylidene); 120.4 (5-C); 129.3, 133.6, 135.3, 139.4, 146.5, 157.7 (Cq arom); 148.3 (C=N); 165.0, 166.5 (C=O). Anal. Calcd for $C_{31}H_{24}N_2O_4S$: C, 71.52; H 4.65; N, 5.38. Found: C, 71.36; H, 4.51; N, 5.54.

5.1.7. 4-{[5-(4-Benzyloxybenzylidene)-4-oxo-2-phenyliminothiazolidin-3-yl]methyl}benzoic acid (4d)

Yield 42%; mp 276–279 °C; ^{1}H NMR ($CDCl_3$): δ 4.90 (s, 2H, OCH_2); 5.02 (s, 2H, NCH_2); 6.77–7.22 (m, 14H, arom); 7.37 (m, 2H, arom); 7.52 (m, 2H, CH); 7.82 (m, 2H, arom); ^{13}C NMR (DMSO-d_6): δ 45.9 (NCH_2); 70.0 (OCH_2); 116.1, 121.5, 125.3, 128.1, 128.2, 128.4, 128.9, 129.9, 130.0, 131.3, 132.3 (CH arom and CH methylidene); 118.3 (5-C); 126.4, 130.5, 136.9, 141.4, 148.1, 160.3 (Cq arom); 150.1 (C=N); 166.3, 167.5 (C=O). Anal. Calcd for $C_{31}H_{24}N_2O_4S$: C, 71.52; H, 4.65; N, 5.38. Found: C, 71.41; H, 4.68; N, 5.24.

5.1.8. 4-[(5-Naphthalen-1-ylmethylene-4-oxo-2-phenyliminothiazolidin-3-yl)methyl] benzoic acid (4e)

Yield 28%; mp 252–255 °C; ^{1}H NMR ($CDCl_3$): δ 5.32 (s, 2H, NCH_2), 6.99–8.19 (m, 16H, arom); 8.56 (s, 1H, CH); ^{13}C NMR (DMSO-d_6): δ 46.2 (NCH_2); 121.4, 123.8, 125.4, 126.0, 126.6, 127.2, 127.8, 128.1, 128.2, 129.3, 129.9, 130.1, 130.9 (CH arom and CH methylidene); 125.0 (5-C); 130.5, 130.9, 131.3, 133.7, 141.3, 147.9 (Cq arom); 150.2 (C=N); 165.7, 167.4 (C=O). Anal. Calcd for $C_{28}H_{20}N_2O_3S$: C, 72.39; H, 4.34; N, 6.03. Found: C, 72.53; H, 4.48; N, 5.89.

5.1.9. 4-[(5-Naphthalen-2-ylmethylene-4-oxo-2-phenyliminothiazolidin-3-yl)methyl] benzoic acid (4f)

Yield 56%; mp 264–266 °C; ^{1}H NMR ($CDCl_3$): δ 5.12 (s, 2H, NCH_2); 6.92–7.97 (m, 17H, arom and CH methylidene); ^{13}C NMR (DMSO-d_6): δ 46.1 (NCH_2), 121.5, 125.6, 126.1, 127.6, 128.2, 128.3, 129.1, 139.4, 130.0, 131.1, 131.2, 131.5 (CH arom and CH methylidene); 121.7 (5-C); 130.7, 131.3, 133.2, 133.6, 141.3, 147.9 (Cq arom); 149.4 (C=N); 166.2, 167.3 (C=O). Anal. Calcd for $C_{28}H_{20}N_2O_3S$: C, 72.39; H, 4.34; N, 6.03. Found: C, 72.18; H, 4.21; N, 6.21.

5.1.10. 4-{[5-(3-Hydroxybenzylidene)-4-oxo-2-phenyliminothiazolidin-3-yl]methyl}benzoic acid (4g)

Yield 67%; mp 280–282 °C; ^{1}H NMR (DMSO-d_6): δ 5.16 (s, 2H, NCH_2); 6.81–7.41 (m, 9H, arom); 7.44 (m, 2H, arom); 7.70 (s, 1H,

CH); 7.94 (m, 2H, arom); 9.80 (br s, 1H, OH); ^{13}C NMR (DMSO-d_6): δ 46.1 (NCH_2); 115.9, 118.0, 121.5, 121.9, 125.5, 128.1, 130.0, 130.1, 130.9, 131.6 (CH arom and CH methylidene); 121.2 (5-C); 130.5, 134.9, 141.4, 148.0, 158.3 (Cq arom); 150.1 (C=N); 166.3, 167.5 (C=O). Anal. Calcd for $C_{24}H_{18}N_2O_4S$: C, 66.96; H, 4.21; N, 6.51. Found: C, 70.15; H, 4.13; N, 6.41.

5.1.11. 4-[5-(4-Hydroxybenzylidene)-4-oxo-2-phenyliminothiazolidin-3-ylmethyl]benzoic acid (4h)

Yield 62%; mp 260–262 °C; ^{1}H NMR ($CDCl_3$): δ 5.08 (s, 2H, NCH_2); 6.75 (m, 2H, arom); 6.85 (m, 2H, arom); 7.06–7.23 (m, 5H, arom); 7.43 (m, 2H, arom); 7.58 (s, 1H, CH); 7.89 (m, 2H, arom); ^{13}C NMR (DMSO-d_6): δ 46.1 (NCH_2); 116.8, 121.4, 125.3, 128.0, 129.9, 130.0, 131.3, 132.7 (CH arom and CH methylidene); 124.6, 130.5, 141.5, 148.1, 160.1 (Cq arom); 150.2 (C=N); 166.4, 167.4 (C=O). Anal. Calcd for $C_{24}H_{18}N_2O_4S$: C, 66.96; H, 4.21; N, 6.51. Found: C, 70.08; H, 4.33; N, 6.37.

5.1.12. 4-[5-(3-Hydroxy-4-methoxybenzylidene)-4-oxo-2-phenyliminothiazolidin-3-ylmethyl]benzoic acid (4i)

Yield 48%; mp 213–216 °C; ^{1}H NMR ($CDCl_3$): δ 3.93 (s, 3H, OCH_3); 5.17 (s, 2H, NCH_2); 6.94–7.36 (m, 8H, arom); 7.56 (m, 2H, arom); 7.65 (s, 1H, CH); 7.97 (m, 2H, arom); 9.81 (s, 1H, OH); ^{13}C NMR (DMSO-d_6): δ 46.1 (NCH_2); 56.2 (OCH_3); 113.0, 116.0, 121.5, 124.0, 125.4, 128.1, 130.0, 130.1, 131.9 (CH arom and CH methylidene); 126.4 (5-C); 117.9, 130.7, 135.7, 141.4, 147.4, 148.2 (Cq arom); 150.4 (C=N); 166.5, 167.6 (C=O). Anal. Calcd for $C_{25}H_{20}N_2O_5S$: C, 65.2; H, 4.38; N, 6.08. Found: C, 65.35; H, 4.19; N, 5.97.

5.1.13. 4-[5-(4-Hydroxy-3-methoxybenzylidene)-4-oxo-2-phenyliminothiazolidin-3-ylmethyl]benzoic acid (4j)

Yield 43%; mp 214–218 °C; ^{1}H NMR ($CDCl_3$): δ 3.89 (s, 3H, OCH_3); 5.26 (s, 2H, NCH_2); 6.93–7.39 (m, 8H, arom); 7.63 (m, 2H, arom); 7.73 (s, 1H, CH); 8.06 (m, 2H, arom); ^{13}C NMR (DMSO-d_6): δ 42.5 (NCH_2); 56.2 (OCH_3); 116.0, 117.2, 121.6, 123.7, 125.6, 127.6, 129.0, 130.1, 132.3 (CH arom and CH methylidene); 124.7 (5-C); 132.1, 135.5, 139.2, 148.3, 161.3, 161.6 (Cq arom); 148.6 (C=N); 166.5, 168.8 (C=O). Anal. Calcd for $C_{25}H_{20}N_2O_5S$: C, 65.2; H, 4.38; N, 6.08. Found: C, 65.28; H, 4.44; N, 5.89.

5.1.14. 4-[5-(3-Carboxy-4-hydroxybenzylidene)-4-oxo-2-phenyliminothiazolidin-3-ylmethyl]benzoic acid (4k)

Yield 20%; mp 280–284 °C; ^{1}H NMR (DMSO-d_6): δ 5.16 (s, 2H, NCH_2); 6.97 (m, 3H, arom); 7.21 (m, 1H, arom); 7.38–7.65 (m, 5H, arom); 7.77 (s, 1H, CH); 7.95 (m, 3H arom); ^{13}C NMR (DMSO-d_6): δ 46.2 (NCH_2); 118.8, 121.4, 125.4, 128.1, 129.9, 130.1, 131.0, 132.8, 136.8, (CH arom and CH methylidene); 115.4, 118.4, 124.3, 130.5, 141.4, 148.0, 163.3 (Cq arom + 5-C); 150.0 (C=N); 166.4, 167.4, 171.2 (C=O). Anal. Calcd for $C_{25}H_{18}N_2O_6S$: C, 63.28; H, 3.82; N, 5.9. Found: C, 63.12; H, 4.00; N, 5.77.

5.2. Molecular modeling

All protein alignments, protein and ligand preparations, and docking studies were performed using the Schrödinger Suite 2007, including Maestro 8.0, Glide 4.5, and Prime 1.6[41] on a PC equipped with a 2.13 GHz Core 2 Duo processor and 3 GB of RAM, running Fedora Core 8 Linux.

Pharmacophore feature detection was performed with LigandScout v2.02,[44] which was also used to create the graphics in Figures 3 and 4.

5.3. Enzyme section

The complete coding sequences of IF1, IF2, Ltp1 LMW-PTPs and PTP1B were cloned in frame with the sequence of the glutathione *S*-transferase (GST) in the pGEX-2T bacterial expression vector. Enzyme expression and purification were achieved in the *Escherichia coli* TB1 strain. Briefly, the recombinant fusion proteins were purified from bacterial lysate using a single step affinity chromatography on glutathione-Sepharose. The solution contained purified fusion proteins were treated with thrombin for 3 h at 37 °C. Then the enzymes were purified from GST and thrombin by gel filtration on Superdex G-75. The purity of proteins preparations were analyzed by SDS–polyacrylamide gel electrophoresis according to Laemmli.[45]

5.3.1. Phosphatase assay and inhibition experiments

Phosphatase assay was carried out at 37 °C using *p*-nitrophenylphosphate as substrate; the final volume was 1 ml. The assay buffer (pH 7.0) contained 0.075 M of β,β-dimethylglutarate buffer, 1 mM EDTA and 5 mM dithiothreitol. The reactions were initiated by addition of aliquots of the enzyme preparations and stopped at appropriate times by adding 4 ml of 1 M KOH. The released *p*-nitrophenolate ion was determined by reading the absorbance at 400 nm (ε = 18,000 M^{-1} cm^{-1}). The main kinetic parameters (K_m and V_{max}) were determined by measuring the initial rates at different substrate concentrations. Experimental data were analysed using the Michaelis equation and a non-linear fitting program (FigSys). Inhibition constants were determined measuring initial hydrolysis rates at differing substrate and inhibitor concentrations. The apparent K_m values measured at the various inhibitor concentrations were plotted against concentration of the inhibitor to calculate the K_i values. All initial rate measurements were carried out in triplicate. For each inhibitor, IC_{50} was determined by measuring the initial hydrolysis rate under fixed *p*-nitrophenylphosphate concentration, equal to the K_m value of the considered PTP. Data were fitted to the following equation using the FigSys program: $V_i/V_0 = IC_{50}/(IC_{50} + [I])$, where V_i is the reaction rate when the inhibitor concentration is [I], V_0 is the reaction rate with no inhibitor, and $IC_{50} = K_i + K_i[S]/K_m$. Therefore, when the substrate concentration [S] is equal to K_m, $IC_{50} = 2K_i$.

Acknowledgements

Work supported in part by FIRB 2003-project RBNE03FMCJ_007, by 'Ente Cassa di Risparmio di Firenze' and by University of Messina (PRA-2005).

Supplementary data

Supplementary data associated with this article can be found, in the online version, at doi:10.1016/j.bmc.2009.01.044.

References and notes

1. Zhang, Z. Y. *Curr. Opin. Chem. Biol.* **2001**, *5*, 416.
2. Zhang, Z. Y.; Zhou, B.; Xie, L. *Pharmacol. Ther.* **2002**, *93*, 307.
3. van Huijsduijnen, R. H.; Bombrun, A.; Swinnen, D. *Drugs Discovery Today* **2002**, *7*, 1013.
4. Tabernero, L.; Aricescu, A. R.; Jones, E. Y.; Szedlacsek, S. E. *FEBS J.* **2008**, *275*, 867.
5. Alonso, A.; Sasin, J.; Bottini, N.; Friedberg, I.; Friedberg, I.; Osterman, A.; Godzik, A.; Hunter, T.; Dixon, J.; Mustelin, T. *Cell* **2004**, *117*, 699.
6. Hendriks, W. J. A.; Elson, A.; Harroch, S.; Stoker, A. W. *FEBS J.* **2008**, *275*, 816.
7. Johnson, T. O.; Ermolieff, J.; Jirousek, M. R. *Nat. Rev. Drug Disc.* **2002**, *1*, 696.
8. (a) Cheng, A.; Uetani, N.; Simoncic, P. D.; Chaubey, V. P.; Lee-Loy, A.; McGlade, J.; Kennedy, B. P.; Tremblay, M. L. *Dev. Cell* **2002**, *2*, 497; (b) Zabolotny, J. M.; Bence-Hanulec, K. K.; Stricker-Krongrad, A.; Haj, F.; Wang, Y.; Minokoshi, Y.; Kim, Y. B.; Elmquist, J. K.; Tartaglia, L. A.; Kahn, B. B.; Neel, B. G. *Dev. Cell* **2002**, *2*, 489.
9. Montalibet, J.; Kennedy, B. P. *Drug Discov. Today Ther. Strategies* **2005**, *2*, 129.
10. Koren, S.; Fantus, I. G. *Best Pract. Res. Cl. En. Metab.* **2007**, *21*, 621.
11. Elchebly, M.; Payette, P.; Michaliszyn, E.; Cromlish, W.; Collins, S.; Loy, A. L.; Normandin, D.; Cheng, A.; Himms-Hagen, J.; Chan, C.; Ramachandran, C.; Gresser, M. J.; Tremblay, M. L.; Kennedy, B. P. *Science* **1999**, *283*, 1544.
12. Klaman, L. D.; Boss, O.; Peroni, O. D.; Kim, J. K.; Martino, J. L.; Zabolotny, J. M.; Moghal, N.; Lubkin, M.; Kim, Y. B.; Sharpe, A. H.; Stricker-Krongrad, A.; Shulman, G. I.; Neel, B. G.; Kahn, B. B. *Mol. Cell. Biol.* **2000**, *20*, 5479.

13. Zhang, S.; Zhang, Z. Y. *Drug Discov. Today* **2007**, *12*, 373.
14. (a) Eckel, R. H.; Grundy, S. M.; Zimmet, P. Z. *Lancet* **2005**, *365*, 1415; (b) Hafner, S. M. *Am. J. Med.* **2006**, *119*, 3S.
15. Jiang, Z. X.; Zhang, Z. Y. *Cancer Metastasis Rev.* **2008**, *27*, 263.
16. Julien, S. G.; Dube, N.; Read, M.; Penney, J.; Paquet, M.; Han, Y.; Kennedy, B. P.; Muller, W. J.; Tremblay, M. L. *Nature Genet.* **2007**, *39*, 338.
17. Chiarugi, P.; Cirri, P.; Marra, F.; Raugei, G.; Camici, G.; Manao, G.; Ramponi, G. *Biochem. Biophys. Res. Commun.* **1997**, *238*, 676.
18. Taddei, M. L.; Chiarugi, P.; Cirri, P.; Talini, D.; Camici, G.; Manao, G.; Raugei, G.; Ramponi, G. *Biochem. Biophys. Res. Commun.* **2000**, *270*, 564.
19. Pandey, S. K.; Yu, X. X.; Watts, L. M.; Michael, M. D.; Sloop, K. W.; Rivard, A. R.; Leedom, T. A.; Manchem, V. P.; Samadzadeh, L.; McKay, R. A.; Monia, B. P.; Bhanot, S. *J. Biol. Chem.* **2007**, *282*, 14291.
20. Kikawa, K. D.; Vidale, D. R.; van Etten, R. L.; Kinch, M. S. *J. Biol. Chem.* **2002**, *277*, 39274.
21. Chiarugi, P.; Taddei, M. L.; Schiavone, N.; Papucci, L.; Giannoni, E.; Fiaschi, T.; Capaccioli, S.; Raugei, G.; Ramponi, G. *Oncogene* **2004**, *23*, 3905.
22. Malentacchi, F.; Marzocchini, R.; Gelmini, S.; Orlando, C.; Serio, M.; Ramponi, G.; Raugei, G. *Biochem. Biophys. Res. Commun.* **2005**, *334*, 875.
23. Lee, S.; Wang, Q. *Med. Res. Rev.* **2007**, *27*, 553.
24. Murthy, V. S.; Kulkarni, V. M. *Bioorg. Med. Chem.* **2002**, *10*, 897.
25. Xin, Z.; Liu, G.; Abad-Zapatero, C.; Pei, Z.; Szczepankiewicz, B. G.; Li, X.; Zhang, T.; Hutchins, C. W.; Hajduk, P. J.; Ballaron, S. J.; Stashko, M. A.; Lubben, T. H.; Trevillyan, J. M.; Jirousek, M. R. *Bioorg. Med. Chem. Lett.* **2003**, *13*, 3947.
26. Burke, T. R.; Lee, K. *Acc. Chem. Res.* **2003**, *36*, 426.
27. Andersen, H. S.; Olsen, O. H.; Iversen, L. F.; Sorensen, A. L. P.; Mortensen, S. B.; Christensen, M. S.; Branner, S.; Hansen, T. K.; Lau, J. F.; Jeppesen, L.; Moran, E. J.; Su, J.; Bakir, F.; Judge, L.; Shahbaz, M.; Collins, T.; Vo, T.; Newman, M. J.; Ripka, W. C.; Moller, N. P. H. *J. Med. Chem.* **2002**, *45*, 4443.
28. Liu, G.; Szczepankiewicz, B. G.; Pei, Z.; Janowick, D. A.; Xin, Z.; Hajduk, P. J.; Abad-Zapatero, C.; Liang, H.; Hutchins, C. W.; Fesik, S. W.; Ballaron, S. J.; Stashko, M. A.; Lubben, T.; Mika, A. K.; Zinker, B. A.; Trevillyan, J. M.; Jirousek, M. R. *J. Med. Chem.* **2003**, *46*, 2093.
29. Zhao, H.; Liu, G.; Xin, Z.; Serby, M. D.; Pei, Z.; Szczepankiewicz, B. G.; Hajduk, P. J.; Abad-Zapatero, C.; Hutchins, C. W.; Lubben, T. H.; Ballaron, S. J.; Haasch, D. L.; Kaszubska, W.; Rondinone, C. M.; Trevillyan, J. M.; Jirousek, M. R. *Bioorg. Med. Chem. Lett.* **2004**, *14*, 5543.
30. Shrestha, S.; Bhattarai, B. R.; Lee, K. H.; Cho, H. *Bioorg. Med. Chem.* **2007**, *15*, 6535.
31. Han, Y.; Belley, M.; Bayly, C. I.; Colucci, J.; Dufresne, C.; Giroux, A.; Lau, C. K.; Leblanc, Y.; McKay, D.; Therien, M.; Wilson, M. C.; Skorey, K.; Chan, C. C.; Scapin, G.; Kennedy, B. P. *Bioorg. Med. Chem. Lett.* **2008**, *18*, 3200.
32. Maccari, R.; Paoli, P.; Ottanà, R.; Jacomelli, M.; Ciurleo, R.; Manao, G.; Steindl, T.; Langer, T.; Vigorita, M. G.; Camici, G. *Bioorg. Med. Chem.* **2007**, *15*, 5137.
33. Puius, Y. A.; Zhao, Y.; Sullivan, M.; Lawrence, D. S.; Almo, S. C.; Zhang, Z. *Proc. Natl. Acad. Sci. U.S.A.* **1997**, *94*, 13420.
34. Scapin, G.; Patel, S. B.; Becker, J. W.; Wang, Q.; Desponts, C.; Waddleton, D.; Skorey, K.; Cromlish, W.; Bayly, C.; Therien, M.; Gauthier, J. Y.; Li, C. S.; Lau, C. K.; Ramachandran, C.; Kennedy, B. P.; Asante-Appiah, E. *Biochemistry* **2003**, *42*, 11451.
35. Ottanà, R.; Maccari, R.; Barreca, M. L.; Bruno, G.; Rotondo, A.; Rossi, A.; Chiricosta, G.; Di Paola, R.; Sautebin, L.; Cuzzocrea, S.; Vigorita, M. G. *Bioorg. Med. Chem.* **2005**, *13*, 4243.
36. Bruno, G.; Costantino, L.; Curinga, C.; Maccari, R.; Monforte, F.; Nicolò, F.; Ottanà, R.; Vigorita, M. G. *Bioorg. Med. Chem.* **2002**, *10*, 1077.
37. Wang, S.; Tabernero, L.; Zhang, M.; Harms, E.; Van Etten, R. L.; Stauffacher, C. V. *Biochemistry* **2000**, *39*, 1903.
38. Bleasdale, J. E.; Ogg, D.; Palazuk, B. J.; Jacob, C. S.; Swanson, M. L.; Wang, X. Y.; Thompson, D. P.; Conradi, R. A.; Mathews, W. R.; Laborde, A. L.; Stuchly, C. W.; Heijbel, A.; Bergdahl, K.; Bannow, C. A.; Smith, C. W.; Svensson, C.; Liljebris, C.; Schostarez, H. J.; May, P. D.; Stevens, F. C.; Larsen, S. D. *Biochemistry* **2001**, *40*, 642.
39. Zhang, M.; Stauffacher, C. V.; Lin, D.; Van Etten, R. L. *J. Biol. Chem.* **1998**, *273*, 21714.
40. Zabell, A. P.; Schroff, A. D.; Bain, B. E.; Van Etten, R. L.; Wiest, O.; Stauffacher, C. V. *J. Biol. Chem.* **2006**, *281*, 6520.
41. *Schrödinger Suite* 2007; Schrödinger, LLC; New York, NY, USA, 2007.
42. Sherman, W.; Day, T.; Jacobson, M. P.; Friesner, R. A.; Farid, R. *J. Med. Chem.* **2006**, *49*, 534.
43. Maccari, R.; Ottanà, R.; Ciurleo, R.; Rakowitz, D.; Matuszczak, B.; Laggner, C.; Langer, T. *Bioorg. Med. Chem.* **2008**, *16*, 5840.
44. (a) Wolber, G.; Dornhofer, A.; Langer, T. *J. Comput. Aided. Mol. Des.* **2006**, *20*, 773; (b) Wolber, G.; Langer, T. *J. Chem. Inf. Comput. Sci.* **2005**, *45*, 160; c *LigandScout 2.02*; Inte:Ligand GmbH, Vienna, Austria, 2008.
45. Laemmli, U. K. *Nature* **1970**, *227*, 680.